BASIC RESEARCH PAPER

Autophagy 11:10, 1821–1832; October 2015; © 2015 Taylor & Francis Group, LLC

Autophagy supports color vision

Zhenqing Zhou, Frans Vinberg, Frank Schottler, Teresa A Doggett, Vladimir J Kefalov, and Thomas A Ferguson*

Department of Ophthalmology and Visual Sciences; Washington University in St. Louis; School of Medicine; St. Louis, MO USA

Keywords: autophagy, color vision, cones, degeneration, photoreceptors, retina

Abbreviations: AMD, age-related macular degeneration; AMPK, AMP-activated protein kinase; ATG5, autophagy-related 5; CIS, cone inner segment; COS, cone outer segment; ERG, electroretinogram; GFP, green fluorescent protein; LC3B, microtubule-associated protein 1 light chain 3 β; LCA, Leber's congenital amaurosis; L/D, 12 h light/12 h dark; ONL, outer nuclear layer; OS, outer segment; p-AMPK, phosphorylated AMPK; PARK2/Parkin, parkin RBR ubiquitin protein ligase; PFA, paraformaldehyde; PINK1, PTEN-induced putative kinase 1; PNA, peanut agglutinin; ROS, reactive oxygen species; RP, retinitis pigmentosa; TEM, transmission electron microscopy; TOMM20/TOM20, translocase of outer mitochondrial membrane 20 homolog (yeast)

Cones comprise only a small portion of the photoreceptors in mammalian retinas. However, cones are vital for color vision and visual perception, and their loss severely diminishes the quality of life for patients with retinal degenerative diseases. Cones function in bright light and have higher demand for energy than rods; yet, the mechanisms that support the energy requirements of cones are poorly understood. One such pathway that potentially could sustain cones under basal and stress conditions is macroautophagy. We addressed the role of macroautophagy in cones by examining how the genetic block of this pathway affects the structural integrity, survival, and function of these neurons. We found that macroautophagy was not detectable in cones under normal conditions but was readily observed following 24 h of fasting. Consistent with this, starvation induced phosphorylation of AMPK specifically in cones indicating cellular starvation. Inhibiting macroautophagy in cones by deleting the essential macroautophagy gene *Atg5* led to reduced cone function following starvation suggesting that cones are sensitive to systemic changes in nutrients and activate macroautophagy to maintain their function. ATG5-deficiency rendered cones susceptible to light-induced damage and caused accumulation of damaged mitochondria in the inner segments, shortening of the outer segments, and degeneration of all cone types, revealing the importance of mitophagy in supporting cone metabolic needs. Our results demonstrate that macroautophagy supports the function and long-term survival of cones providing for their unique metabolic requirements and resistance to stress. Targeting macroautophagy has the potential to preserve cone-mediated vision during retinal degenerative diseases.

Introduction

The loss of postmitotic rod and cone photoreceptors is a common feature of inherited retinal diseases such as retinitis pigmentosa (RP). Many degenerative diseases of the retina begin with the loss of rods followed by the progressive loss of cones.[1,2] Attempts to preserve vision by inhibiting cell death[3,4] or gene replacement[5-7] have met with varying degrees of success; unfortunately treatments that are universally effective are not available. An alternative strategy for preserving photoreceptors that could be used in conjunction with other methods might be to augment survival pathways such as macroautophagy (hereafter autophagy). Autophagy is now recognized as a crucial survival pathway activated in response to cellular stress, and a protective role for autophagy has been proposed against a number of neurodegenerative diseases.[8-11] Autophagy has been implicated in a wide variety of physiological processes related to cancer, metabolism, immunity, and aging.[12] Furthermore, autophagy functions under basal conditions to remove damaged cellular constituents and it supports the daily metabolic requirements of cells by providing sources of energy and building blocks. Mitophagy, an autophagy-related process, prevents cell damage and maintains energy supplies by continuously removing oxidatively damaged mitochondria.[13,14] In the eye, autophagy has been detected during retinal degeneration,[1,4] retinal injury[15] and light stress.[16,17] A noncanonical autophagy pathway supports photoreceptor outer segment phagocytosis and the classical visual cycle in the retinal pigment epithelium (RPE).[18]

The retina is one of the most metabolically active tissues in the body, utilizing glucose as the primary energy source. Changes in metabolism brought about by restricting glucose can lead to visual dysfunction and even retinal degeneration.[19,20] The importance of insulin signaling[1,21,22] to the survival of the cone photoreceptors suggests that boosting metabolism might be an effective therapeutic approach. Given that autophagy is intimately tied to the metabolic requirements of all cells, stimulating this pathway in the retina might prove efficacious. However, the precise role of

*Correspondence to: Thomas A Ferguson; Email: ferguson@vision.wustl.edu
Submitted: 03/04/2015; Revised: 08/11/2015; Accepted: 08/12/2015
http://dx.doi.org/10.1080/15548627.2015.1084456

autophagy in the metabolism and long-term function of the retina is not understood.

The loss of cone photoreceptor function is particularly devastating to patients with degenerative eye diseases as cones are critical for color vision and visual perception in daytime light conditions. In the blinding eye disease age-related macular degeneration (AMD), it is the loss of the cones that diminishes the quality of life for patients.[23] Cones function in bright light and must generate more ATP compared to rods[19,24,25] suggesting that they may have their own unique metabolic requirements that could be supported by increasing autophagy. Unfortunately cones represent only a small portion of the total photoreceptors in mice and humans making cone-specific therapies challenging. Moreover, little is known about the function of autophagy in cones due to the lack of available tools to assess this pathway. Here we investigate the role of autophagy in cones by examining autophagy-deficient cone photoreceptors under normal and stress conditions.

Results

Starvation-induced autophagy in cone photoreceptors

A major function of autophagy is stress survival[12] as demonstrated by the robust induction of this pathway in mouse tissues during starvation.[26] Considering the metabolic needs of the retina[19] and the high energy requirements of cone photoreceptors,[25,27,28] we hypothesized that the retina might be sensitive to acute changes in systemic metabolism. We addressed this by examining the retina of the GFP-LC3 reporter mouse strain following 24 h of fasting. GFP-LC3 expression was diffuse prior to starvation (**Fig. 1A**); however, after mice were fasted for 24 h GFP-LC3 expression was detectable in the cone inner and outer segments (**Fig. 1B**, arrows). That this was related to autophagy was confirmed when the GFP-LC3 mouse was crossed to a mouse strain in which the essential autophagy gene *Atg5* was deleted specifically in cone photoreceptors (called the *Atg5*$^{\Delta Cone}$ strain, see Materials and Methods for details). This abolished the starvation-induced accumulation of GFP-LC3 in the cones (**Fig. 1C**, arrowheads). Transmission electron microscopy (TEM) confirmed the GFP-LC3 findings where autophagosomes were not observed in control mice (no starvation; **Fig. 1D**); but were evident in the cone outer segments following starvation (**Fig. 1E**). Autophagosomes were never observed in the cones of *Atg5*$^{\Delta Cone}$ mice even under starvation conditions (**Fig. 1F**). A further indication that the cones were sensitive to systemic starvation was the phosphorylation of the energy sensor AMPK in the cones of control mice following starvation (**Fig. 1G**, right panel, arrows). Activated AMPK was not detected in ATG5-deficient cones either before or after starvation (**Fig. 1H**, left and right panels, respectively). Neither increased GFP-LC3 nor phosphorylated AMPK were detected in rods under any conditions even when the retina was examined throughout the daily L/D cycle (not shown). In addition, changes in GFP-LC3 expression were not observed in other layers of the retina following starvation (**Fig. S1A-C**) verifying that cones are uniquely sensitive in this situation.

The activation of autophagy in cones by starvation suggested that cones may utilize this pathway during periods of systemic nutrient

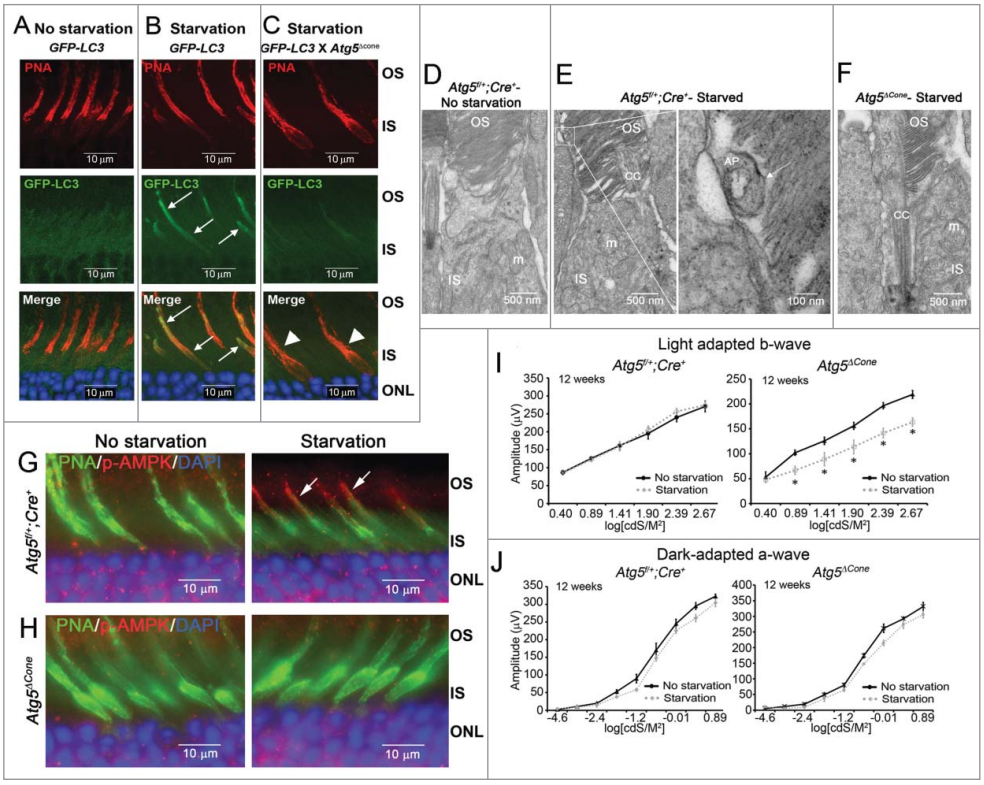

Figure 1. Starvation-induced GFP-LC3 accumulation in the cones. (**A-C**) Representative confocal images of retinae from 25-wk-old GFP-LC3 transgenic mice. (**A**) GFP-LC3 mice, No starvation (n = 3 mice per treatment). (**B**) GFP-LC3 mice, starvation (n = 3 mice per treatment). (**C**) GFP-LC3 x *Atg5*$^{\Delta Cone}$ mice, starvation. GFP-LC3 (green) (n = 3 mice per treatment), PNA (red), DAPI (nuclei, blue). (**D-F**) Representative electron micrographs from 12-wk-old *Atg5*$^{f/+}$;*Cre*$^{+}$ and *Atg5*$^{\Delta Cone}$ (n = 2 per group). (**D**) *Atg5*$^{f/+}$;*Cre*$^{+}$, no starvation. (**E**) *Atg5*$^{f/+}$;*Cre*$^{+}$, starvation; with enlarged image of an autophagosome (AP). (**F**) *Atg5*$^{\Delta Cone}$, starvation. OS, outer segment; IS, inner segment; m, mitochondria; CC, connecting cilium. (**G-H**) Representative confocal images of retina (n = 4–6 retina examined per group) from 12-wk-old mice stained for phospho (p-)AMPK. (**G**) *Atg5*$^{f/+}$; *Cre*$^{+}$. (**H**) *Atg5*$^{\Delta Cone}$. (**I**) Light adapted b-wave responses for 12-wk-old *Atg5*$^{f/+}$;*Cre*$^{+}$ (n = 4) and *Atg5*$^{\Delta Cone}$ (n = 5) mice with and without starvation. (**J**) Dark-adapted b-wave responses for *Atg5*$^{f/+}$;*Cre*$^{+}$ (n = 4) and *Atg5*$^{\Delta Cone}$ (n = 3) mice with and without starvation (*p < 0.05).

deprivation to maintain function. We tested this idea by examining the effect of starvation on cone function in the presence or absence of ATG5. Although starvation had no discernable effect on light-adapted b-wave responses in control mice (**Fig. 1I**, left panel), it significantly diminished cone function in the *Atg5*$^{\Delta Cone}$ strain (**Fig. 1I**, right panel). Starvation had no effect on rod function either in control or *Atg5*$^{\Delta Cone}$ mice (**Fig. 1J**). Loss of cone function in ATG5-deficient cones was not the result of cone cell death as there was no reduction in cone numbers following starvation (**Fig. S1D**). Thus, the starvation-induced activation of autophagy is unique to cones following 24-h fasting and is important for maintaining their function during periods of systemic nutrient imbalance.

Light-induced stress in cone photoreceptors

Light exposure can generate significant oxidative stress in photoreceptors and is particularly harmful in certain mouse strains harboring a leucine at amino acid 450 in the RPE65 protein.[29] Our mouse strains were generated on the C57BL/6J background that is resistant to light damage due to a methionine at amino acid 450 in RPE65.[29,30] Nevertheless, cones are typically resistant to light damage without accompanying rod cell damage.[30] One explanation for this observation could be that autophagy protects cones against the damaging effects of intense light. We examined this idea by exposing 12-wk-old *Atg5*$^{\Delta Cone}$ and littermate control (*Atg5*$^{f/+}$;*Cre*$^{+}$) mice to light of 13,000 lx for 7 h before returning them to normal lighting (12 h L/D cycle) for 1 wk. Cone numbers were then assessed in the mid-dorsal and ventral regions by PNA staining of retinal flat mounts. Following intense light exposure cone numbers in control mouse retinae were unaffected (**Fig. 2A**, *Atg5*$^{f/+}$;*Cre*$^{+}$); however, there was a substantial loss of cones in the dorsal region of the *Atg5*$^{\Delta Cone}$ retina (**Fig. 2A**). The ventral region was less affected consistent with the observation that light stress preferentially affects the superior region of the retina.[30] Importantly, whereas control mouse cones were unaffected by light stress (**Fig. 2B**, right panel), the morphology of both M- and S-cones in the mid dorsal region of *Atg5*$^{\Delta Cone}$ retinae was markedly altered (**Fig. 2C**, right panel) compared to *Atg5*$^{\Delta Cone}$ retinae that were not exposed to intense light (**Fig. 2C**, left panel). Light induced a substantial shortening of the M- and S-cone outer segments (**Fig. 2C**, right panel, arrowheads) as well as swelling of inner segments. Because mitochondria are heavily localized to the cone inner segments[31] we examined the expression of TOMM20/TOM20 (translocase of outer mitochondrial membrane 20 homolog [yeast]), a mitochondrial marker located on the mitochondrial membrane that is part a complex that regulates the translocation of proteins into the mitochondria.[13] We found significant labeling of the inner segments of *Atg5*$^{\Delta Cone}$ cones after light stress (**Fig. 2E**, right panel, arrowheads). Interestingly, increased TOMM20 staining (red) was noted in *Atg5*$^{\Delta Cone}$ cones even before light stress was applied (**Fig. 2E**, left panel, arrows) implying *Atg5* deletion may be affecting cone mitochondria. It is notable that this light intensity had no discernable effect on retinal morphology in control or *Atg5*$^{\Delta Cone}$ mice indicating that the rods were not overtly affected (**Fig. 2F and 2G**).

Defective mitophagy in ATG5-deficient cones

Increased TOMM20 expression in the cone inner segments in the *Atg5*$^{\Delta Cone}$ retina (**Fig. 2E**) suggested effects on the mitochondria and prompted us to examine the cone inner segments of *Atg5*$^{\Delta Cone}$ mice more closely. First, we observed that, similar to

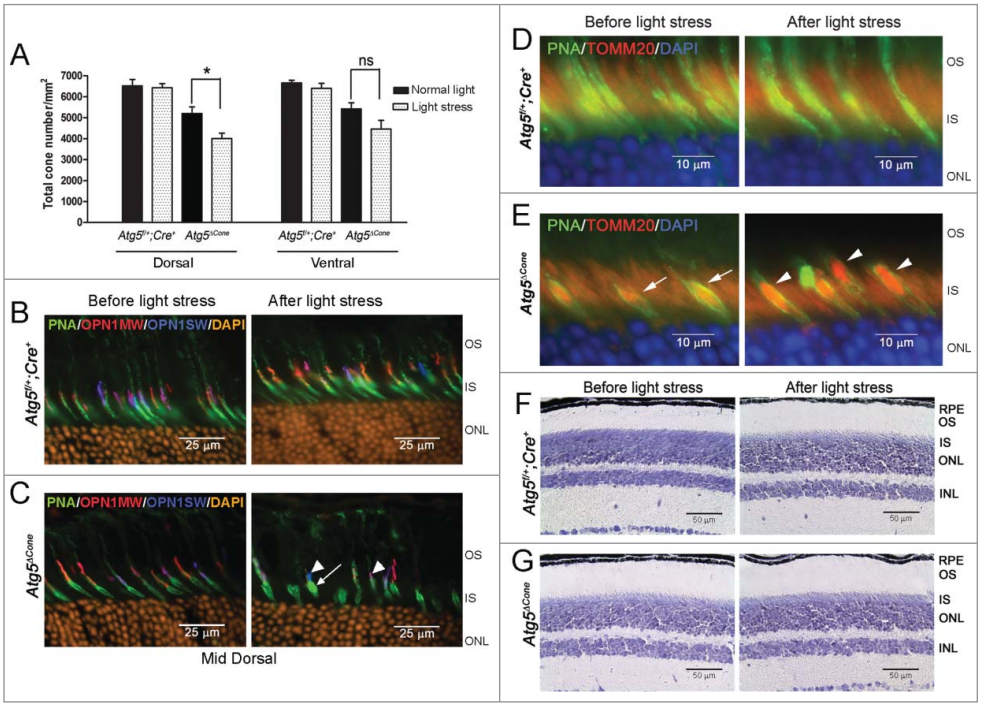

Figure 2. Light-induced damage to ATG5-deficient cone photoreceptors. (**A**) Twelve-wk-old *Atg5*$^{f/+}$;*Cre*$^{+}$ control (n = 4) and *Atg5*$^{\Delta Cone}$ mice (n = 5) were exposed to 13,000 lx for 7 h and returned to normal lighting for 1 wk. Cone counts performed on retinal flat mounts. Data represent the mean ± standard error. * denotes significantly different from control ($p < 0.05$); ns, not significant. (**B**) and (**C**) Representative confocal images of *Atg5*$^{f/+}$;*Cre*$^{+}$ (**B**) and *Atg5*$^{\Delta Cone}$ (**C**) retinae before and after light stress stained for PNA (green), OPN1MW/M-opsin (red), OPN1SW/S-opsin (blue), and DAPI (orange). (**D**) and (**E**) Representative confocal images of *Atg5*$^{f/+}$;*Cre*$^{+}$ (**D**) and *Atg5*$^{\Delta Cone}$ (**E**) retinae before and after light stress stained for PNA (green), TOMM20 (red), and DAPI (blue). (**F**) and (**G**). Representative images of *Atg5*$^{f/+}$;*Cre*$^{+}$ (**F**) and *Atg5*$^{\Delta Cone}$ (**G**) retinae before and after light stress stained with toluidine blue. RPE, retinal pigmented epithelium; OS, outer segment; IS, inner segment; ONL, outer nuclear layer; INL, inner nuclear layer. (n = 4–6 retina examined per group)

TOMM20, SQSTM1/p62 was concentrated to swollen inner segments (**Fig. 3A**, right panel, arrows). SQSTM1 is an autophagy receptor protein that interacts directly with the cargo to be degraded and is required both for the formation and autophagic degradation of polyubiquitin-containing bodies. The accumulation of SQSTM1 is a common feature following disruption of autophagy in many tissues.[32-35] TEM examination of the cone inner segments (CIS) (**Fig. 3B-E**) revealed that ATG5-deficient cones contained many mitochondrial profiles (**Fig. 3D**, CIS) compared to control (**Fig. 3B**, CIS). Whereas mitochondria in control mice exhibited regularly spaced and densely packed cristae (**Fig. 3C**, arrowheads) the mitochondria in the CIS of *Atg5*$^{\Delta Cone}$ mice were electron lucent with sparse and irregularly arranged cristae (**Fig. 3E**, arrows). Morphometric analysis of the electron micrographs revealed that although the inner segment length did not change (**Fig. 3F**), the total area of the inner segments was increased compared to controls at 12 wk of age, with a further increase by 29 wk (**Fig. 3G**). In addition, the mitochondrial area in the inner segments was also increased at 12 wk; and substantially more so by 29 wk (**Fig. 3H**) implying that damaged mitochondria were accumulating over time. Consistent with the mitochondrial damage observed in the inner segments was the presence of reactive oxygen species (ROS) in the *Atg5*$^{\Delta Cone}$ cones (**Fig. 3I**, right panel,

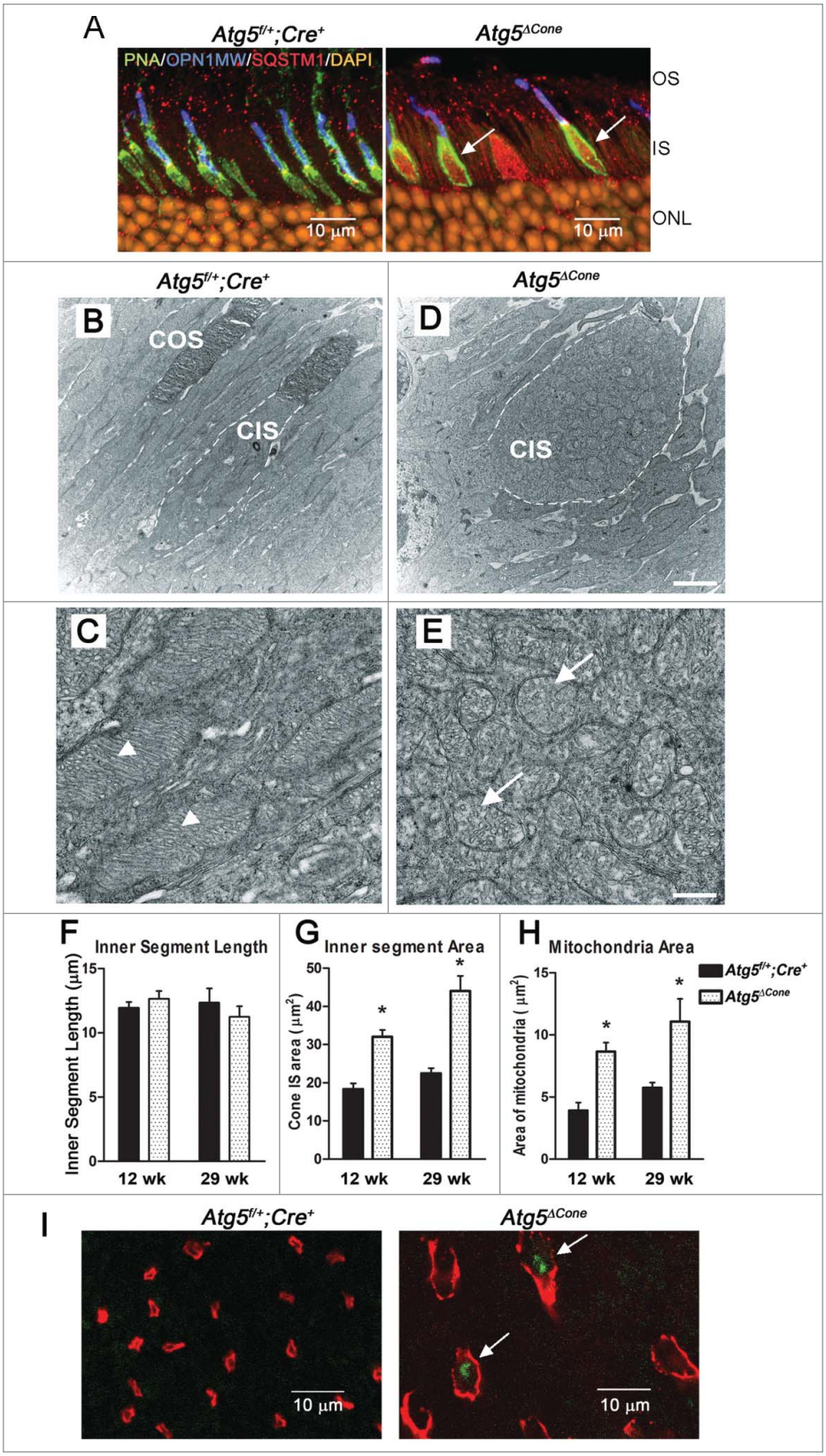

Figure 3. Analysis of the inner segments of ATG5-deficient cones. (**A**) Representative confocal images of retina (n = 6 retina examined per group) from 24-wk-old *Atg5*$^{f/+}$;*Cre*$^{+}$ and *Atg5*$^{\Delta Cone}$ mice stained for SQSTM1 (red, arrows); PNA (green), OPN1MW/M-opsin (blue) and nuclei (orange). OS, outer segment; IS, inner segment; ONL, outer nuclear layer. (**B-E**), TEM analysis of cone inner segment morphology in the retinae of control (*Atg5*$^{f/+}$;*Cre*$^{+}$) (**B**, **C**) and *Atg5*$^{\Delta Cone}$ (**D**, **E**) mice at 29 wk of age. Calibration Bars: (**B**, **D**) = 2 μm; (**C**, **E**) = 0.5 μm. Dashed line indicates outline of CIS. CIS, cone inner segment; COS, cone outer segment. (**F**) Quantitative analysis of cone inner segment length from TEM micrographs taken at 12 wk and 29 wk. (**G**) Cone inner segment area from TEM micrographs taken at 12 wk and 29 wk. (**H**) Mitochondrial area from TEM micrographs taken at 12 wk and 29 wk. * denotes significantly different from control ($p<0.05$), n = 4. (**I**) Representative confocal images of live retinal explants from *Atg5*$^{f/+}$; *Cre*$^{+}$ and *Atg5*$^{\Delta Cone}$ mice staining for ROS, arrows; PNA (red) and DHR123 (ROS, green).

arrows) compared to controls (**Fig. 3I**, left panel) demonstrating that oxidatively damaged mitochondria were present. (Note that the swollen inner segments are very prominent in this micrograph, compare **Fig. 3I** left vs. right panels.) A further indication of mitochondrial damage in *Atg5*$^{\Delta Cone}$ inner segments was revealed when we observed increased staining for the E3-ubiquitin (Ub) ligase PARK2 (**Fig. S2A**) and the mitochondrial kinase PINK1 (**Fig. S2B**).

Loss of cone photoreceptors following deletion of *Atg5*

Functional and morphological changes in ATG5-deficient cones in response to starvation and bright light demonstrate that cones rely heavily on this pathway during periods of stress. However, the presence of damaged mitochondria in ATG5-deficient cones without stress (**Fig. 3**) suggested that autophagy might have an important role in the long-term survival of these neurons even under basal conditions as damaged mitochondria could indicate an energy deficit. Accordingly, we enumerated cone cell numbers at various time points between 8 and 40 wk of age in control and *Atg5*$^{\Delta Cone}$ mice from retinal flat mounts that were stained for PNA. Although cone cell numbers remained relatively constant up to 8 wk of age, there was a 15–20% reduction in total cone cells in *Atg5*$^{\Delta Cone}$ mice by 14 wk (**Fig. 4A**). Over the ensuing weeks there was a gradual decline in cone numbers such that by 40 wk they were reduced by >90%. This analysis also revealed that both M- cones and S-cones were lost in the *Atg5*$^{\Delta Cone}$ mouse retina and this was evident in the dorsal, ventral, nasal, and temporal regions of the eye. The representative immunofluorescence micrographs shown in **Fig. 4B and 4C** (stained for OPN1MW/M-opsin, OPN1SW/S-opsin and PNA) from the mid-dorsal and ventral regions of the retina highlight these findings. At 18 wk the swollen inner segments were prominent in both OPN1MW/M-opsin (red, **Fig. 4B**, upper right panel, arrowheads) and OPN1SW/S-opsin cones (blue, **Fig. 4C**, upper right panel, arrowheads). At 40 wk cone numbers from both regions were significantly diminished (**Fig. 4B**, lower right panel; **Fig. 4C**, lower right panel). In addition, cone loss in the *Atg5*$^{\Delta Cone}$ mice was independent of daily light exposure as animals maintained in constant darkness from 4 wk until they were 40 wk of age (final time point in **Fig. 4A**) lost similar numbers of cone photoreceptors compared to controls (**Fig. S3**).

Progressive changes in degenerating ATG5-deficient cones

Swollen inner segments were observed as early as 7 wk in *Atg5*$^{\Delta Cone}$ mice (**Fig. 4E**, left panel, *) compared to control (**Fig. 4D**, left panel) indicating that this may be an early morphological change in ATG5-deficient cones. At 7 wk outer segment lengths were similar between *Atg5*$^{\Delta Cone}$ and control mice (**Fig. 5F**); but subsequent measurements revealed a gradual reduction progressing with age in the *Atg5*$^{\Delta Cone}$ mice compared to controls (**Fig. 4F**). By 51 wk only remnants of the outer segments of the OPN1MW/M-opsin^{+} and OPN1SW/S-opsin^{+} cones were detectable in the *Atg5*$^{\Delta Cone}$ mice (**Fig. 4E**, right panel, arrowheads), whereas cones in control retinae were unchanged (**Fig. 4D**, right panel). Thus, the loss of autophagy in cones leads to the accumulation of damaged mitochondria in the inner segments (**Fig. 3**); followed by progressive shortening of the outer segments and eventually the complete loss of these cells (**Fig. 4**).

Compromised cone signaling in *Atg5*$^{\Delta Cone}$ mice

We also performed electroretinogram (ERG) recordings to determine whether the deletion of *Atg5* affected phototransduction and signaling of cones. By using ex vivo ERG analysis from isolated retinae[36] we found that at 12 wk both control (*Atg5*$^{fl+}$; *Cre*$^{+}$) and *Atg5*$^{\Delta Cone}$ cones responded robustly to light (**Fig. 5A and B**). However, the maximum amplitude of *Atg5*$^{\Delta Cone}$ cones was on average 43% smaller than that of control cones (inset in **Fig. 5C**). The significantly decreased amplitude cannot be explained by the slightly reduced cone number alone (see **Fig. 4**), suggesting that the transduction channel current of individual ATG5-deficient cones was also somewhat reduced at this age. The reason for that is not clear but the damaged mitochondria and swollen inner segments (see **Fig. 2-4**) that were already evident at 12 wk of age, as well as possible slight shortening of the outer segments (**Fig. 4**), might have contributed to the reduced amplitudes. Interestingly, the amplitudes normalized with the maximal response amplitude elicited by the brightest flash in each retina were not statistically different between control and *Atg5*$^{\Delta Cone}$ mice (**Fig. 5C**). The fractional sensitivity (see Materials and Methods and **Fig. 5C**) of ATG5-deficient cones appeared somewhat reduced but the difference was not statistically significant. We next wanted to follow how cone signaling (both phototransduction and synaptic transmission) were affected by the deletion of *Atg5* in aging mice that experience the gradual death of cones. For this, we determined cone b-wave amplitudes by *in vivo* ERG. We found that the reduction of maximum b-wave amplitude in aging mice (**Fig. 5F**) correlated well with the reduced number of cones in *Atg5*$^{\Delta Cone}$ mice (**Fig. 4A**). Thus, deletion of *Atg5* does not seem to directly affect phototransduction or the synaptic transmission of dark-adapted cones beyond their reduced numbers. This conclusion is further supported by the lack of a significant effect of *Atg5* deletion on the fractional sensitivity of cone signaling, as determined from the b-waves normalized with the maximal response amplitude to the brightest flash in aging mice (**Fig. 5D and 5E**). The cone-driven responses in 32-wk-old *Atg5*$^{\Delta Cone}$ mice were too small to allow rigorous quantitative analysis most likely due to the progressive cone degeneration (see **Fig. 4A**). Together, our ERG results demonstrate that cone function is normal in 8-wk-old *Atg5*$^{\Delta Cone}$ mice but becomes suppressed by wk 12 and progressively degrades as mice age due to the loss of cones.

Rod signaling in *Atg5*$^{\Delta Cone}$ mice

In contrast to the gradually degenerating cones, the structure of the rods in the retina of *Atg5*$^{\Delta Cone}$ mice appeared normal even at 52 wk (**Fig. 6A**, right panel), and there was no obvious reduction in outer nuclear layer (ONL) nuclei (**Fig. 6B**). Consistent with the normal rod structure, the rod-driven scotopic a-waves of 8-wk and 18-wk-old mice were comparable in *Atg5*$^{\Delta Cone}$ and control mice (**Fig. 6C**, left and center panels, respectively). However, we found that at 32 wk the rod-driven responses were significantly reduced (**Fig. 6C**, right panel). This result was surprising

considering the normal morphology of the rods at that age. To determine whether the cone-specific deletion of *Atg5* somehow affected the function of rods, we recorded flash responses from individual rods using a suction electrode. In contrast to the in vivo ERG recordings, single-cell recordings did not reveal statistically significant changes in maximal response amplitude (R_{max}: 14 ± 0.1 pA in control and 13 ± 0.4 pA in $Atg5^{\Delta Cone}$ mice, n = 26) or sensitivity ($E_{1/2}$: 17 ± 1 photons μm^{-2} in control and 15 ± 1 photons μm^{-2} in $Atg5^{\Delta Cone}$ mice, n = 26) of rods in $Atg5^{\Delta Cone}$ mice, even in 52-wk-old mice. Furthermore, the rod response waveforms appeared similar between the 52-wk-old control and $Atg5^{\Delta Cone}$ mice (**Fig. 6D**). Thus, progressive cone degeneration in $Atg5^{\Delta Cone}$ mice appeared to have no significant impact on rod photoreceptors. The suppression in the scotopic in vivo ERG voltage response may reflect structural changes in the retina affecting its resistance.

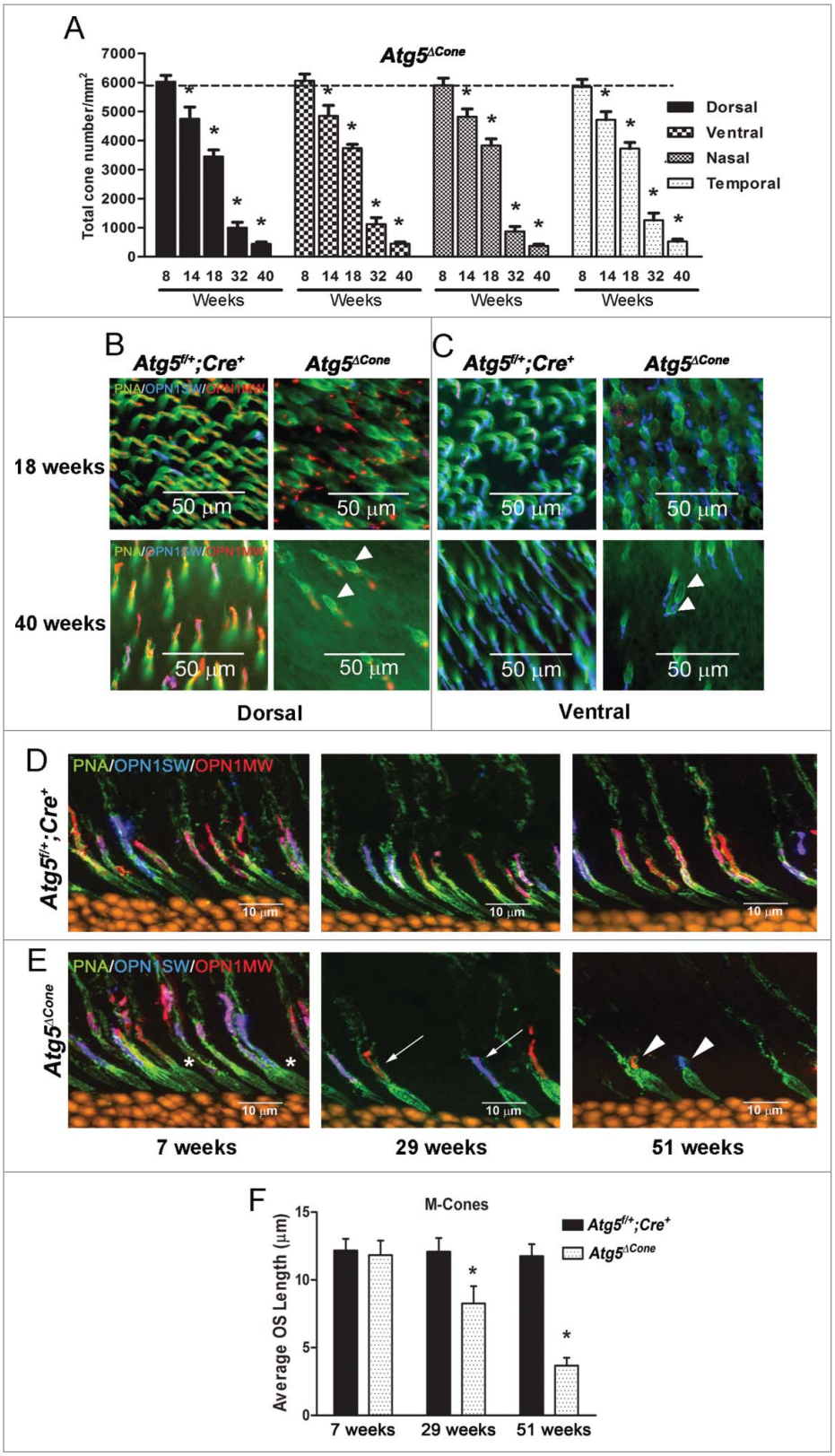

Discussion

Cells require continuous intercellular recycling by the autophagy pathway to generate energy and building blocks under both physiological and stress

Figure 4. Degeneration of ATG5-deficient cones. (**A**) Mouse retinae from $Atg5^{f/+};Cre^{+}$ (n = 4 for each time point) and $Atg5^{\Delta Cone}$ mice (n = 4 for each time point) were harvested at various ages and cones were enumerated following staining of retinal flat mounts for PNA (green), OPN1MW/M-opsin (red) and OPN1SW/S-opsin (blue). Data represent the mean ± standard error, * denotes statistically different ($p < 0.05$) from control which is represented by the dotted line (cone numbers averaged from all control mice = 5884 ± 48). (**B**) Representative confocal micrographs of the dorsal region of the retina from $Atg5^{f/+};Cre^{+}$ (left panels) and $Atg5^{\Delta Cone}$ mice (right panels) taken at 18 wk (upper panels) and 40 wk (lower panels) (n = 4–6 retina examined per group). (**C**) Representative confocal micrographs of the ventral region of the retina from $Atg5^{f/+};Cre^{+}$ (left panels) and $Atg5^{\Delta Cone}$ mice (right panels) taken at 18 wk (upper panels) and 40 wk (lower panels) (n = 4–6 retina examined per group). Representative confocal images of the retinae of control $Atg5^{f/+}$; Cre^{+} (**D**) and $Atg5^{\Delta Cone}$ (**E**) mice at 7, 29, and 51 wk illustrating the loss of both M (red) and S (blue) cones in $Atg5^{\Delta Cone}$ mice. PNA (green) and nuclei (orange), n = 4–6 retina examined per group. (**F**) M-cone outer segment length of $Atg5^{f/+}$; Cre^{+} and $Atg5^{\Delta Cone}$ mice at 7, 29, and 51 wk. Data represent the mean ± standard error, * denotes statistically significant from control ($p < 0.05$), n = 4 for each time point.

conditions. In post-mitotic cells autophagy is particularly important as these cells must maintain function under a variety of conditions without the possibility of regeneration.[12,34,35] Photoreceptors are terminally differentiated and would be expected to rely on autophagy for their long-term survival. Indeed, our recent work determined that without autophagy rod photoreceptors lose function and degenerate.[37] Though other studies have also addressed the role of autophagy in rods,[16,38] little is known about this process in cones. Cones are far less abundant than rods but are essential for visual acuity, making their loss especially devastating to patients with degenerative eye diseases.[1,2,23] Here we have examined the importance of autophagy in cones with the idea that this pathway could eventually be the target of therapeutic intervention. Our results show that by activating autophagy cones survive and maintain their function during periods of systemic nutritional imbalance and during light stress. In addition, cones rely heavily on mitophagy to retain the healthy mitochondria necessary to supply their high energy needs. Together these results indicate that cone photoreceptors utilize autophagy to accommodate their unique physiological requirements under basal and stress conditions.

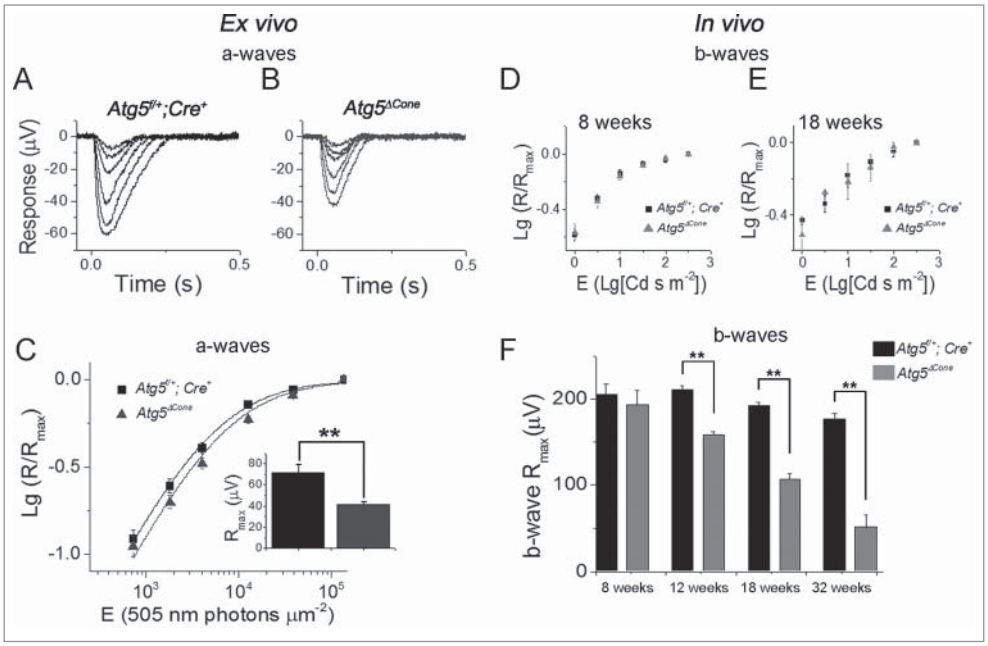

Figure 5. Response to light stimuli in ATG5-deficient cones. (**A-C**) Ex vivo ERG responses. Cone a-wave responses in 12-wk-old *Atg5*$^{f/+}$; *Cre*$^{+}$ control (A) and *Atg5*$^{\Delta Cone}$ mice (**B**). (**C**) Logarithmic normalized a-wave response amplitudes (R/R_{max})) from ex vivo ERG experiments plotted as a function of E for control and *Atg5*$^{\Delta Cone}$ mice (mean ± SEM, n = 16 control and 16 *Atg5*$^{\Delta Cone}$ retinas, **denotes significantly different from control, p = 0.003). Equation 1 with $E_{1/2}$ of 5,400 and 6,900 photons μm^{-2} described the amplitude data of control and *Atg5*$^{\Delta Cone}$ mice (least squares fitting), respectively. (**D-F**) Logarithmic normalized cone b-wave amplitudes from in vivo ERG recordings plotted as a function of flash energy for 8- (**D**) and 18- (**E**) wk-old control and *Atg5*$^{\Delta Cone}$ mice. (**F**) The maximal amplitudes at 8, 12, 18, and 32 wk for control (Atg5$^{f/+}$;Cre^{+}) and *Atg5*$^{\Delta Cone}$ mice are shown. ** denotes significantly different from control, $p < 0.05$ (n = 5).

The retina requires a constant supply of glucose to sustain its high rate of metabolism and maintain function.[19,39] Changes in metabolism brought on by long-term hypoglycemia can affect vision and lead to degeneration of photoreceptors.[20,40,41] Whereas rod and cone vision can both be affected by restricting glucose,[20,42] other studies have shown that rods are more sensitive than cones to hypoglycemia[24,43] implicating an additional mechanism in cones that resists the effects of reduced glucose. In the mouse, 24 h of fasting reduces serum glucose and insulin levels[44] and in response tissues activate autophagy to support their energy requirements.[26] Our results show that cones are also uniquely sensitive to systemic starvation and respond by activating autophagy, likely brought about by the activation of AMPK. AMPK is a sensor of the energy state of a cell brought on by decreases in intracellular ATP and increases in the AMP:ATP ratio.[45] It is noteworthy that ATG5-deficient cones do not phosphorylate AMPK in response to starvation suggesting that there may be insufficient ATP (and thus AMP) to stimulate this response. The critical nature of the autophagic response to cones was further supported by our results showing loss of function in ATG5-deficient cones following starvation. This loss of function was in the absence of measurable cone cell death suggesting that autophagy supports the function of cones under starvation conditions. Thus, when glucose availability is limited cones utilize autophagy to mobilize energy-rich compounds to produce energy and maintain function. Although the raw material used by cones during starvation is not known, rodent cones possess glycogen stores.[46] In addition, primate cones (but not rods) can use endogenous glycogen sources to generate glucose for energy production.[24] It is notable that rods do not respond to 24-h fasting by phosphorylating AMPK or activating autophagy indicating that the autophagy is not utilized by rods in this situation.

Healthy mitochondria are essential for cellular homeostasis as they are the sites of ATP production through oxidative phosphorylation. A byproduct of the respiratory chain is the production of ROS that can cause oxidative damage to the mitochondrial lipids, proteins, and DNA leading to mitochondrial damage and cellular dysfunction.[13] Accumulation of damaged mitochondria is prevented by their continuous fission and fusion which permits the segregation and clearance of dysfunctional mitochondria through mitophagy.[47] Thus, it is not surprising that cells with high energy demands such as cones would rely heavily on mitophagy as their increased metabolism and ATP requirements would produce excess ROS potentially damaging their mitochondria. Our observation that the earliest feature of ATG5-deficiency in cones was

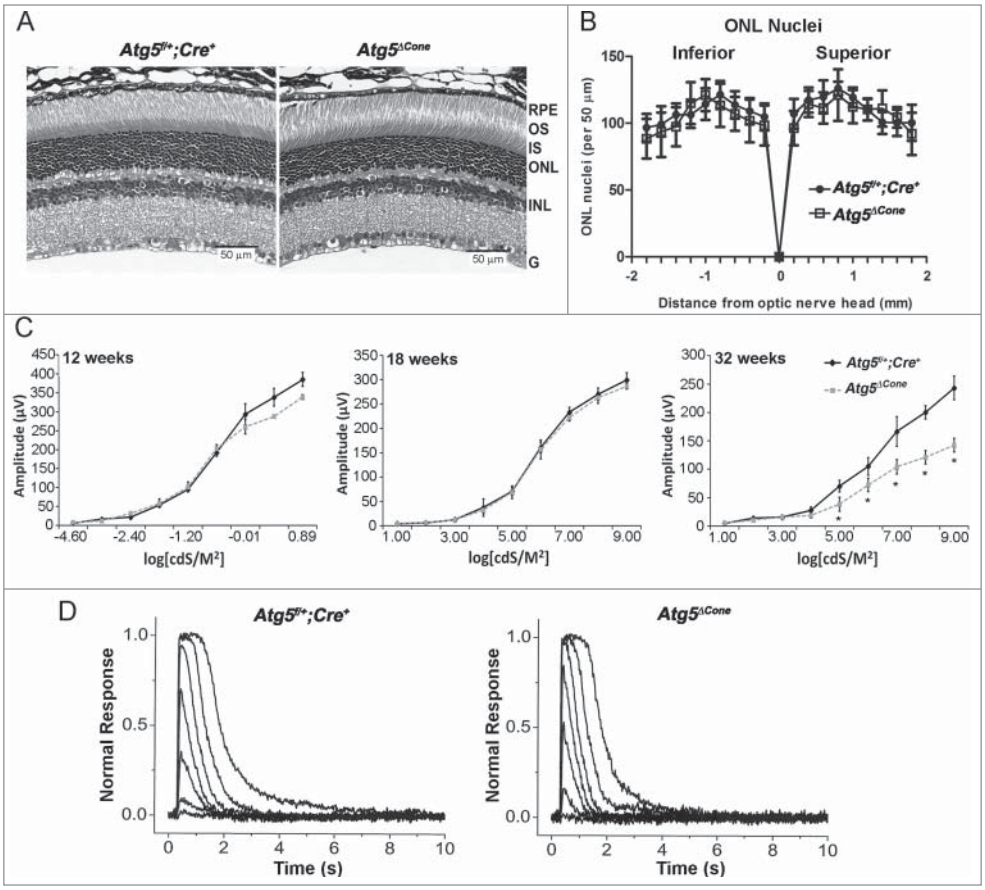

Figure 6. Analysis of rod function in *Atg5*$^{\Delta Cone}$ mice. (**A**) Retinal sections from *Atg5*$^{f/+}$; *Cre*$^{+}$ (left) and *Atg5*$^{\Delta Cone}$ (right) mice at 52 wk. (**B**) Outer nuclear layer nuclei density in *Atg5*$^{f/+}$; *Cre*$^{+}$ and *Atg5*$^{\Delta Cone}$ mice at 54 wk. (**C**) Comparison of rod in vivo ERG a-wave response amplitudes from *Atg5*$^{f/+}$; *Cre*$^{+}$ control) and *Atg5*$^{\Delta Cone}$ mice at 8 wk (left), 18 wk (middle), and 32 wk (right). * denotes significantly different from control, $p < 0.05$, $n = 5$. (**D**) Representative flash response families from *Atg5*$^{f/+}$; *Cre*$^{+}$ control (left) and *Atg5*$^{\Delta Cone}$ (right) mice at 52 wk. Flash intensities range from 0.9 to 1297 photons μm^{-2} in ~0.5 log unit increments.

the accumulation of damaged mitochondria in the inner segments supports this idea. In addition, the increased energy demands during light stress would also necessitate efficient regulation of mitochondrial fitness and explains why intense light accelerated mitochondrial damage in ATG5-deficient cones.

It is well established that cones continue to function in bright light[48] and are very resistant to direct damage by very intense light exposure. In fact, when cone damage is observed it is secondary to changes in the rods.[30] Our findings show that without autophagy, cones are directly susceptible to light damage even when the rods are unaffected. Thus, in intense light autophagy operates as an endogenous protective mechanism for cones permitting them to maintain structure and function. Our observation of light-induced cone degeneration in the *Atg5*$^{\Delta Cone}$ mouse retina is particularly striking as the ATG5-deficiency is present in the C57BL6/J background, a strain resistant to the damaging effect of intense light. Previous studies have established that susceptibility of the retina to light stress is associated with a polymorphism in the RPE protein RPE65. Strains with leucine at amino acid position 450 (e.g., BALB/c) are susceptible to light damage, whereas those with a methionine at that position (e.g.,, C57BL/6) are resistant.[29] Susceptibility is related to the rapid rate of rhodopsin regeneration via the RPE visual cycle and degeneration occurs due to the buildup of toxic byproducts from this pathway. Resistant strains regenerate rhodopsin at a much slower pace, which does not allow the accumulation of toxins and subsequent retinal damage. That cones degenerate in the presence of the resistant phenotype in the *Atg5*$^{\Delta Cone}$ strain further highlights the importance of ATG5–mediated autophagy as an endogenous survival pathway for cones. It further suggests that cones may be directly damaged by light independent of the visual cycle. In sharp contrast, we recently reported that rods do not utilize autophagy in the same capacity, as ATG5-deficient rods in the resistant C57BL6/J background were completely resistant to the level of intense light used in the current studies.[37]

Finally, our results demonstrate that although autophagy is important for cone survival, it does not directly modulate cone signaling. We observed normal cone b-wave responses in 8-wk-old mice prior to the onset of degeneration, demonstrating that the deletion of *Atg5* does not directly affect cone-mediated signaling in the retina. The subsequent progressive loss in photopic responses in *Atg5*$^{\Delta Cone}$ mice could be attributed to the gradual loss of cone cells with advancing age. The fractional sensitivity of cones as determined from normalized a- or b-wave amplitudes was also unaffected in ATG5-deficient cones, even in mice older than 8 wk. This suggests that the fraction of transduction channels closed and the relative change in transmitter release at the cone synapse by unit stimulation is not dependent on ATG5 even in aging mice. The eventual decrease in rod function was surprising considering that the deletion of *Atg5* was restricted only to the cones. However, rod dysfunction following the cone-specific deletion of critical molecules has been reported in patients with cone dystrophy[49] and CNGB3 achromatosia.[50] Loss of rod function induced by cone degeneration has also been reported in mice, including *Gnat2*^{cpfl3},[51] *Cnga3*$^{-/-}$,[52] and *Ranbp2*$^{-/-}$[53] strains. Deletion of the gene encoding the PtdIns3K subunit PIK3R1/p85α in cones also results in some loss of rod function but, similar to our findings, these authors did not observe rod cell death; they speculated that synaptic

changes in cones may have affected rod function.[21] We think this is unlikely in our case, as we observed suppression in the rod-driven a-wave, which is generated upstream of the synapse. The normal responses produced by individual rods from *Atg5*$^{\Delta Cone}$ mice indicate that the scotopic ERG defect was not intrinsic to the rods, but likely reflected altered retinal resistance induced by the cone degeneration.

Our results demonstrate that cone photoreceptors utilize autophagy to support their physiology and function in a variety of circumstances. Their unique requirements for autophagic mechanisms to support resistance to environmental stress, changes in systemic metabolism, and long-term survival distinguishes them from rods and indicates that directly boosting this survival pathway in cones might be an effective therapy. Strategies to increase autophagy in a number of disease states have been recently discussed[54] and such approaches could be used alone or in combination with other modalities to prevent the loss of vision in blinding eye disorders.

Materials and Methods

Mouse strains

HRGP-Cre transgenic mice, in which Cre recombinase is controlled by a fragment of the promoters from the human red (*OPN1LW*) and green (*OPN1MW2*) pigment genes (referred to as *HRGP*; generously provided by Dr. Y.Z. Le, University of Oklahoma Health Sciences Center)[55] were crossed to the *Atg5*$^{flox/flox}$ mice (generously provided by Dr. Noboru Mizushima, Tokyo Medicine and Dental University, Tokyo, Japan) to generate the *Atg5*$^{\Delta Cone}$ mouse line in which *Atg5* was specifically deleted in cone cells. *Atg5*$^{\Delta Cone}$ offspring are born viable, in reasonable numbers, and do not show any developmental defects in the eye or other organs at birth (data not shown). Cre recombinase expression in cones was confirmed by staining retinal cryosections with PNA Alexa Fluor 488 and Cre-antibody (Millipore, 69050). In this strain Cre recombinase expression was observed beginning at p10 as reported[55] (and data not shown) and was strong in all PNA^{+} cells of the retina at 7 wk (**Fig. S4**, arrowheads). In experiments where *Atg5*$^{\Delta Cone}$ and control mice were crossed with GFP-LC3 transgenic mice (generously provided by Dr. Noboru Mizushima) only hemizygous animals were used, as determined by PCR genotyping protocol.[56]

All transgenic and conditional knockout lines were crossed to the C57BL/6J strain (Jackson Labs, strain 000664) and verified as congenic by microsatellite analysis (Research Animal Diagnostic and Investigative Laboratory, RADIL, University of Missouri, Columbia, MO). All strains were free of the *Crb1*^{rd8} mutation by PCR analysis.[57] Mice were housed in a barrier facility operated and maintained by the Division of Comparative Medicine of Washington University School of Medicine. Experiments were carried out in strict accordance with recommendations in the Guide for the Care and Use of Laboratory Animals of the National Institutes of Health (NIH) and in accordance with the ARVO resolution on the use of animals for ophthalmic research. In all experiments littermate control animals were used (*Atg5*$^{f/+}$; *Cre*$^{+}$) and experiments contained at least 3 mice per group. Each experiment was repeated a minimum of 3 times.

Reagents and antibodies

PNA lectin (*Arachis hypogaea*) conjugated to either Alexa Fluor 488 (L2109) or Alexa Fluor 647 (L32460), SlowFade Gold Antifade Reagent with diamidino-2-phenylindole (DAPI; S36938), dihydrorhodamine 123 (DHR 123; D-23086), and RPMI-1640 medium (11875–110) were purchased from Life Technologies; MEM vitamin solution (M6895) and MEM amino acid solution (M5550) were purchased from Sigma-Aldrich. The following antibodies were used: Red/Green OPN1LW/Opsin (Millipore, AB5405); OPN1SW (sc-14363), cone transducin α (sc-390) and TOMM20 (sc-11415), phospho-PRKAA1/AMPK1-PRKAA2/AMPK2 (sc-33524) from Santa Cruz Biotechnology; SQSTM1/p62 (PROGEN Biotechnik Gmbh, GP62-C); anti-rabbit Alexa Fluor 594 (A21207), anti-goat Alexa Fluor 647 (A21447) from Life Technologies; PARK2/Parkin (ab15954), PINK1 (ab23707) from Abcam.

Retinal flat mounts

Enucleated eyes were carefully dissected to remove the retina from the underlying RPE, sclera and choroid and immediately fixed in 4% paraformaldehyde (PFA) in 1X phosphate buffered saline (PBS; Leinco Technologies, P349) for 4 h at 4°C. Retinas were rinsed 3 times with ice-cold PBS and then blocked with donkey serum (Sigma, D9663) for 2 h at room temperature. Retinas were then incubated with primary antibodies and PNA overnight at 4°C, washed with PBS and incubated with fluorescent-labeled secondary antibodies for 2 h at room temperature. Radial cuts (average, 4) were made from the edge of the retinal tissue toward the center of the retina, then flat mounted onto slides with the photoreceptor outer segments facing up. Cone cells were then counted in 3 non-overlapping fields with an area of 0.0616 mm^2, each field at a location midway between the optic nerve head and the retinal margin, using images collected with an Olympus BX51 fluorescence microscope. Data are expressed as average total cone number /mm^2.

Immunofluorescence staining

Enucleated eyes were fixed in 4% PFA overnight at 4°C, transferred to 30% sucrose (Sigma, S9378)/PBS overnight at 4°C and then embedded in O.C.T. Compound (TissueTek, 4583). Sagittal cryosections of 7-μm thickness were cut and placed on polylysine slides (Fisher Scientific, PL400). Sections were briefly rinsed in PBS then placed in blocking buffer (PBS containing 10% donkey serum, 2% BSA (Sigma, A7906), 0.2% Triton X-100 [Sigma, P1379]) for 2 h at room temperature and then incubated with primary antibodies and Alexa Fluor 488-conjugated PNA in dilution buffer (2% donkey serum, 0.2% Triton X-100 in PBS) overnight at 4°C followed by secondary fluorescent-labeled antibodies in dilution buffer for 2 h at room temperature. Nuclei were stained with DAPI present in the mounting medium. In the light stress experiments cryosections were also stained with 0.1% toluidine blue to examine retina morphology before and after stress.

Photoreceptor nuclei enumeration

Photoreceptor nuclei in the outer nuclear layer were counted in sagittal cut cryosections that were stained with the nuclear stain DAPI. Images were captured using an Olympus BX51 fluorescence microscope, and cell nuclei counted using the ImageJ software (NIH) in an area of 50 μm × 50 μm at 200 μm intervals from the optic nerve head in the superior and inferior regions. Data are expressed as the nucleus number/50 μm^2.

Measurement of cone outer segment length

To measure cone outer segment (OS) length sagittal cut cryosections were stained with the OPN1MW/M-opsin antibody, PNA conjugated to Alexa Fluor 488 and nuclear stain DAPI. Images were captured using an Olympus BX51 fluorescence microscope and individual cone OS length measured using the MetaMorph software (Molecular Devices). Data are expressed in average length in μm.

Light stress analysis

Light stress experiments were performed on mice that were dark-adapted overnight. The light source was a fluorescent lamp (Radium Lampenwerk, BioSun NL-T8 36/965/G13) with a lambda max of 500 nm. Prior to light exposure 1% cyclopentolate hydrochloride (Alcon, NDC 0065–0396–05) was administered to temporarily stop the eye from focusing and to dilate the pupil. Pupils were then further dilated with 2.5% phenylephrine hydrochloride (Falcon Pharmaceuticals, 631314–342–01) and the mice were exposed to 13,000 lx of white light for 7 h, with reapplication of phenylephrine every 2 h. The mice were then returned to the normal L/D cycle for 1 wk. Eyes were enucleated and processed for histological analysis.

Dark adaptation

Prolonged dark adaption studies were performed by placing 4-wk-old $Atg5^{fl/+;}Cre^{+}$ and $Atg5^{\Delta Cone}$ mice in a dark room (no white light) until they were 40 wk of age. Cages, water bottles, and food were changed under dim red light.

Reactive oxygen species measurement

Enucleated eyes were carefully dissected to remove the retina from the underlying RPE, sclera and choroid, rinsed in PBS then placed in RPMI-1640 medium with 10% fetal bovine serum, 100 U/ml penicillin, and 100 μg/ml streptomycin and incubated at 37°C with 5% CO_2 for 3 h. Retinal explants were then incubated with Alexa Fluor 647 conjugated to PNA (10 μg/ml) and 10 μM DHR123 for 1 h at 37°C in culture medium, rinsed briefly with PBS and placed in fresh culture medium. Confocal microscopy was performed at 37°C. Live images of the retinal explants were acquired by an inverted confocal laser scanning microscope (Zeiss LSM510 confocal microscope) facilitated with multiline argon lasers (458, 488, and 515 nm), helium/neon red laser (633 nm), helium/neon green laser (543 nm). Images were stored, visualized, and analyzed using the Zeiss Image Browser Program.

In vivo electroretinography

Electroretinograms on $Atg5^{\Delta Cone}$ and age-matched littermate control mice were performed as previously described.[18] Briefly, mice were dark-adapted overnight and anesthetized by intraperitoneal injection of mouse cocktail (86.9 mg/kg ketamine and 13.4 mg/kg xylazine diluted in PBS). After pupil dilation (1% atropine sulfate; AKORN, 17478–215–15), full-field scotopic ERGs were recorded using a Tucker–Davis System 3 Complete ABR/OAE Workstation (Tucker–Davis Technologies). Photopic ERGs were recorded after light adaptation for 10 min.

Ex vivo ERG

Mice were dark-adapted overnight and euthanized by CO_2 inhalation followed by cervical dislocation, and the eyes were enucleated and placed in Locke's medium pH7.4 (112.5 mM NaCl, 3.6 mM KCl, 2.4 mM $MgCl_2$, 1.2 mM $CaCl_2$, 10 mM HEPES, 20 mM $NaHCO_3$, 3 mM Na succinate, 0.5 mM Na glutamate, 0.02 mM EDTA, 10 mM glucose, 0.1% MEM vitamins and amino acids) under dim red light. Retinas were dissected in Locke's medium under IR light by using IR converters attached to the dissection microscope and mounted on the specimen holder[36] in which they were perfused at 3–4 mL/min with Locke's medium. The photoreceptor component of the ERG signal (a-wave) was isolated by adding 40 μM DL-AP4 (Tocris Bioscience, 3699), 2 mM L-aspartate and 100 μM $BaCl_2$ into the perfusion medium. Perfusion solution was continuously bubbled with carbogen (5% CO_2) and maintained at 38°C. Photoreceptors were stimulated with 505-nm light that formed a homogenous spot overfilling the effective Ø0.5 mm recording area of the central retina. Cone responses were isolated by double flash technique[58] by using 88,000 photons (505 nm) μm^{-2} pre-flash (1 ms) followed by varying test flashes ranging from 700 to 14,000 photons μm^{-2} delivered 250 ms after the pre-flash when rods remained still saturated. The ERG signal was amplified by differential amplifier (DP-311, Warner Instruments), sampled at 10 kHz, low-pass filtered at 300 Hz (8-pole Bessel filter) and collected using a digitizer (Digidata 1440A,) and pCLAMP 9 software from Molecular Devices. Response amplitudes at time-to-peak (R) were plotted as a function of flash energy (in photons μm^{-2}) and the half-saturating flash energy ($E_{1/2}$) was determined by fitting a Naka-Rushton function

$$\frac{R}{R_{max}} = \frac{E}{E + E_{1/2}}$$

where R_{max} was the maximal response amplitude of saturated cone response and E test flash energy in photons (505 nm) μm^{-2}. The fractional sensitivity is defined as $1/E_{1/2}$, describing the fraction of light-sensitive current turned off by 1 photon (505 nm) μm^{-2}.[59]

Single rod cell recordings

Light-sensitive current of the rod outer segments was recorded with suction electrodes as described previously.[60] Briefly, retinas were dissected as described above for ex vivo ERG recordings,

cut into small pieces, and transferred into the recording chamber where they were perfused with Locke's solution (see above) at 37°C. Single rod outer segments were drawn into a pipette (containing 140 mM NaCl, 3.6 KCl, 2.4 $MgCl_2$, 1.2 mM $CaCl_2$, 3 mM HEPES, 10 mM glucose, pH 7.4) and light responses to flashes of 500 nm light (calibrated as described above for *ex vivo* ERG recordings) were recorded. Data were acquired at 1000 Hz, low-pass filtered at 30 Hz (8-pole Bessel filter) then collected and analyzed as described above.

Transmission electron microscopy

Mice were deeply anesthetized with Ketamine/Xylazine and fixed by intra-cardiac perfusion with a quick rinse of 0.1% Heparin in 0.1 M sodium phosphate buffer (pH 7.4) followed by 2% PFA/2.5% glutaraldehyde in 0.1 M phosphate buffer (pH 7.35). Eyes were then immersion-fixed overnight, post-fixed in 1% osmium tetroxide for 1 h and stained *en bloc* with 1% uranyl acetate in 0.1 M acetate buffer (pH 7.4) for 2 h. Blocks were then dehydrated in a graded series of ethanol followed by propylene oxide (Electron Microscopy Sciences, 32952), and embedded in Araldite 6005/EMbed 812 resin (Electron Microscopy Sciences). Semi-thin sections (0.5–1 μm) were cut through the entire retina at the level of the optic nerve and stained with toluidine blue. Ultra-thin sections were taken from a 600 to 800 μm length of retina where the majority of inner segments were oriented longitudinally; samples from the same areas were matched between control and experimental animals. Ultra-thin sections were then post-stained with uranyl acetate and lead citrate, viewed on a Hitachi H7500 electron microscope and documented in digital images. Micrographs of all cone inner segments that were continuous with the cone cell bodies were collected from a single section of each animal. Cone inner segment area, length, and the maximum width were measured using Image J software for the analysis of 7–10 micrographs from 3 mice per group.

Statistics

Statistical significance was calculated using a paired 2-tailed t test. Results with $p < 0.05$ were considered statistically significant.

Disclosure of Potential Conflicts of Interest

No potential conflicts of interest were disclosed.

Funding

This work was supported by a National Institutes of Health Grants EY015570 (T.A.F.), EY019312 (V.J.K.), EY02687 (Dept. of Ophthalmology and Visual Science Core Grant), a Department of Ophthalmology and Visual Science grant from Research to Prevent Blindness (New York, NY), The Carl Marshall Reeves and Mildred Almen Reeves Foundation (Columbus, IN), and The BrightFocus Foundation (Clarksburg, MD).

Supplemental Material

Supplemental data for this article can be accessed on the publisher's website.

References

1. Punzo C, Kornacker K, Cepko CL. Stimulation of the insulin/mTOR pathway delays cone death in a mouse model of retinitis pigmentosa. Nat Neurosci 2009; 12:44-52; PMID:19060896; http://dx.doi.org/10.1038/nn.2234
2. Hartong DT, Berson EL, Dryja TP. Retinitis pigmentosa. Lancet 2006; 368:1795-809; PMID:17113430; http://dx.doi.org/10.1016/S0140-6736(06)69740-7
3. Sanges D, Comitato A, Tammaro R, Marigo V. Apoptosis in retinal degeneration involves cross-talk between apoptosis-inducing factor (AIF) and caspase-12 and is blocked by calpain inhibitors. Proc Nat Acad Sci USA 2006; 103:17366-71; PMID:17088543; http://dx.doi.org/10.1073/pnas.0606276103
4. Murakami Y, Matsumoto H, Roh M, Suzuki J, Hisatomi T, Ikeda Y, Miller JW, Vavvas DG. Receptor interacting protein kinase mediates necrotic cone but not rod cell death in a mouse model of inherited degeneration. Proc Nat Acad Sci USA 2012; 109:14598-603; PMID:22908283; http://dx.doi.org/10.1073/pnas.1206937109
5. Cuenca N, Fernandez-Sanchez L, Campello L, Maneu V, De la Villa P, Lax P, Pinilla I. Cellular responses following retinal injuries and therapeutic approaches for neurodegenerative diseases. Prog Retin Eye Res 2014; 43C:17-75; http://dx.doi.org/10.1016/j.preteyeres.2014.07.001
6. Travis GH, Golczak M, Moise AR, Palczewski K. Diseases caused by defects in the visual cycle: retinoids as potential therapeutic agents. Annu Rev Pharmacol Toxicol 2007; 47:469-512; PMID:16968212; http://dx.doi.org/10.1146/annurev.pharmtox.47.120505.105225
7. Bennett J. Gene therapy for color blindness. N Eng J Med 2009; 361:2483-4; http://dx.doi.org/10.1056/NEJMcibr0908643
8. Wong E, Cuervo AM. Autophagy gone awry in neurodegenerative diseases. Nat Neurosci 2010; 13:805-11; PMID:20581817; http://dx.doi.org/10.1038/nn.2575
9. Rivera JF, Costes S, Gurlo T, Glabe CG, Butler PC. Autophagy defends pancreatic β cells from human islet amyloid polypeptide-induced toxicity. J Clin Invest 2014; 124:3489-500; PMID:25036708; http://dx.doi.org/10.1172/JCI71981
10. Schneider JL, Cuervo AM. Autophagy and human disease: emerging themes. Curr Opin Genet Dev 2014; 26C:16-23; http://dx.doi.org/10.1016/j.gde.2014.04.003
11. Nixon RA. The role of autophagy in neurodegenerative disease. Nat Med 2013; 19:983-97; PMID:23921753; http://dx.doi.org/10.1038/nm.3232
12. Mizushima N, Komatsu M. Autophagy: renovation of cells and tissues. Cell 2011; 147:728-41; PMID:22078875; http://dx.doi.org/10.1016/j.cell.2011.10.026
13. Ashrafi G, Schwarz TL. The pathways of mitophagy for quality control and clearance of mitochondria. Cell Death Differ 2013; 20:31-42; PMID:22743996; http://dx.doi.org/10.1038/cdd.2012.81
14. Geisler S, Holmstrom KM, Skujat D, Fiesel FC, Rothfuss OC, Kahle PJ, Springer W. PINK1/Parkin-mediated mitophagy is dependent on VDAC1 and p62/SQSTM1. Nat Cell Biol 2010; 12:119-31; PMID:20098416; http://dx.doi.org/10.1038/ncb2012
15. Besirli CG, Chinskey ND, Zheng Q-D, Zacks DN. Autophagy Activation in the Injured Photoreceptor Inhibits Fas-Mediated Apoptosis. Invest Ophthal Vis Sci 2011; 52:4193-9; PMID:21421874; http://dx.doi.org/10.1167/iovs.10-7090
16. Chen Y, Sawada O, Kohno H, Le YZ, Subauste C, Maeda T, Maeda A. Autophagy Protects the Retina from Light-induced Degeneration. J Biol Chem 2013; 288:7506-18; PMID:23341467; http://dx.doi.org/10.1074/jbc.M112.439935
17. Kunchithapautham K, Coughlin B, Lemasters JJ, Rohrer B. Differential effects of rapamycin on rods and cones during light-induced stress in albino mice. Invest Ophthal Vis Sci 2011; 52:2967-75; PMID:21273550; http://dx.doi.org/10.1167/iovs.10-6278
18. Kim JY, Zhao H, Martinez J, Doggett TA, Kolesnikov AV, Tang PH, Ablonczy Z, Chan CC, Zhou Z, Green DR, et al. Noncanonical autophagy promotes the visual cycle. Cell 2013; 154:365-76; PMID:23870125; http://dx.doi.org/10.1016/j.cell.2013.06.012
19. Chertov AO, Holzhausen L, Kuok IT, Couron D, Parker E, Linton JD, Sadilek M, Sweet IR, Hurley JB. Roles of glucose in photoreceptor survival. J Biol Chem 2011; 286:34700-11; PMID:21840997; http://dx.doi.org/10.1074/jbc.M111.279752
20. Umino Y, Everhart D, Solessio E, Cusato K, Pan JC, Nguyen TH, Brown ET, Hafler R, Frio BA, Knox BE, et al. Hypoglycemia leads to age-related loss of vision. Proc Nat Acad Sci USA 2006; 103:19541-5; PMID:17159157; http://dx.doi.org/10.1073/pnas.0604478104
21. Ivanovic I, Anderson RE, Le YZ, Fliesler SJ, Sherry DM, Rajala RV. Deletion of the p85alpha regulatory subunit of phosphoinositide 3-kinase in cone photoreceptor cells results in cone photoreceptor degeneration. Invest Ophthal Vis Sci 2011; 52:3775-83; PMID:21398281; http://dx.doi.org/10.1167/iovs.10-7139
22. Rajala A, Dighe R, Agbaga MP, Anderson RE, Rajala RV. Insulin receptor signaling in cones. J Biol Chem 2013; 288:19503-15; PMID:23673657; http://dx.doi.org/10.1074/jbc.M113.469064
23. Zarbin MA. Current concepts in the pathogenesis of age-related macular degeneration. Arch Ophthal 2004;

122:598-614; PMID:15078679; http://dx.doi.org/10.1001/archopht.122.4.598
24. Nihira M, Anderson K, Gorin FA, Burns MS. Primate rod and cone photoreceptors may differ in glucose accessibility. Invest Ophthal Vis Sci 1995; 36:1259-70; PMID:7775103
25. Okawa H, Sampath AP, Laughlin SB, Fain GL. ATP consumption by mammalian rod photoreceptors in darkness and in light. Curr Biol 2008; 18:1917-21; PMID:19084410; http://dx.doi.org/10.1016/j.cub.2008.10.029
26. Mizushima N, Yamamoto A, Matsui M, Yoshimori T, Ohsumi Y. *In vivo* analysis of autophagy in response to nutrient starvation using transgenic mice expressing a fluorescent autophagosome marker. Mol Biol Cell 2004; 15:1101-11; PMID:14699058; http://dx.doi.org/10.1091/mbc.E03-09-0704
27. Perkins GA, Ellisman MH, Fox DA. The structure-function correlates of mammalian rod and cone photoreceptor mitochondria: observations and unanswered questions. Mitochondrion 2004; 4:695-703; PMID:16120425; http://dx.doi.org/10.1016/j.mito.2004.07.020
28. Perkins GA, Frey TG. Recent structural insight into mitochondria gained by microscopy. Micron 2000; 31:97-111; PMID:10568232; http://dx.doi.org/10.1016/S0968-4328(99)00065-7
29. Wenzel A, Reme CE, Williams TP, Hafezi F, Grimm C. The Rpe65 Leu450Met variation increases retinal resistance against light-induced degeneration by slowing rhodopsin regeneration. J Neurosci 2001; 21:53-8; PMID:11150319
30. Organisciak DT, Vaughan DK. Retinal light damage: mechanisms and protection. Prog Retin Eye Res 2010; 29:113-34; PMID:19951742; http://dx.doi.org/10.1016/j.preteyeres.2009.11.004
31. Hoang QV, Linsenmeier RA, Chung CK, Curcio CA. Photoreceptor inner segments in monkey and human retina: mitochondrial density, optics, and regional variation. Vis Neurosci 2002; 19:395-407; PMID:12511073; http://dx.doi.org/10.1017/S0952523802194028
32. Klionsky DJ, Abdalla FC, Abeliovich H, Abraham RT, Acevedo-Arozena A, Adeli K, Agholme L, Agnello M, Agostinis P, Aguirre-Ghiso JA, et al. Guidelines for the use and interpretation of assays for monitoring autophagy. Autophagy 2012; 8:445-544; PMID:22966490; http://dx.doi.org/10.4161/auto.19496
33. Hara T, Nakamura K, Matsui M, Yamamoto A, Nakahara Y, Suzuki-Migishima R, Yokoyama M, Mishima K, Saito I, Okano H, et al. Suppression of basal autophagy in neural cells causes neurodegenerative disease in mice. Nature 2006; 441:885-9; PMID:16625204; http://dx.doi.org/10.1038/nature04724
34. Komatsu M, Waguri S, Chiba T, Murata S, Iwata J, Tanida I, Ueno T, Koike M, Uchiyama Y, Kominami E, et al. Loss of autophagy in the central nervous system causes neurodegeneration in mice. Nature 2006; 441:880-4; PMID:16625205; http://dx.doi.org/10.1038/nature04723
35. Hartleben B, Godel M, Meyer-Schwesinger C, Liu S, Ulrich T, Kobler S, Wiech T, Grahammer F, Arnold SJ, Lindenmeyer MT, et al. Autophagy influences glomerular disease susceptibility and maintains podocyte homeostasis in aging mice. J Clin Invest 2010; 120:1084-96; PMID:20200449; http://dx.doi.org/10.1172/JCI39492
36. Vinberg F, Kolesnikov AV, Kefalov VJ. Ex vivo ERG analysis of photoreceptors using an in vivo ERG system. Vision Res 2014; 101:108-17; PMID:24959652; http://dx.doi.org/10.1016/j.visres.2014.06.003
37. Zhou Z, Doggett TA, Sene A, Apte RS, Ferguson TA. Autophagy supports survival and phototransduction protein levels in rod photoreceptors. Cell Death Differ 2015; 22(3):488-98
38. Rodriguez-Muela N, Koga H, Garcia-Ledo L, de la Villa P, de la Rosa EJ, Cuervo AM, Boya P. Balance between autophagic pathways preserves retinal homeostasis. Aging cell 2013; 12:478-88; PMID:23521856; http://dx.doi.org/10.1111/acel.12072
39. Ames A, 3rd, Gurian BS. Effects of glucose and oxygen deprivation on function of isolated mammalian retina. J Neurophysiol 1963; 26:617-34; PMID:14012566
40. Emery M, Schorderet DF, Roduit R. Acute hypoglycemia induces retinal cell death in mouse. PloS one 2011; 6:e21586; PMID:21738719; http://dx.doi.org/10.1371/journal.pone.0021586
41. Zeevalk GD, Nicklas WJ. Lactate prevents the alterations in tissue amino acids, decline in ATP, and cell damage due to aglycemia in retina. J Neurochem 2000; 75:1027-34; PMID:10936183; http://dx.doi.org/10.1046/j.1471-4159.2000.0751027.x
42. Khan MI, Barlow RB, Weinstock RS. Acute hypoglycemia decreases central retinal function in the human eye. Vision Res 2011; 51:1623-6; PMID:21601590; http://dx.doi.org/10.1016/j.visres.2011.05.003
43. Macaluso C, Onoe S, Niemeyer G. Changes in glucose level affect rod function more than cone function in the isolated, perfused cat eye. Invest Ophthal Vis Sci 1992; 33:2798-808; PMID:1526729
44. Ezaki J, Matsumoto N, Takeda-Ezaki M, Komatsu M, Takahashi K, Hiraoka Y, Taka H, Fujimura T, Takehana K, Yoshida M, et al. Liver autophagy contributes to the maintenance of blood glucose and amino acid levels. Autophagy 2011; 7:727-36; PMID:21471734; http://dx.doi.org/10.4161/auto.7.7.15371
45. Egan DF, Shackelford DB, Mihaylova MM, Gelino S, Kohnz RA, Mair W, Vasquez DS, Joshi A, Gwinn DM, Taylor R, et al. Phosphorylation of ULK1 (hATG1) by AMP-activated protein kinase connects energy sensing to mitophagy. Science 2011; 331:456-61; PMID:21205641; http://dx.doi.org/10.1126/science.1196371
46. Okubo A, Sameshima M, Unoki K, Uehara F, Ohba N. Ultracytochemical demonstration of glycogen in cone, but not in rod, photoreceptor cells in the rat retina. Ann Anat 1998; 180:307-14; PMID:9728270; http://dx.doi.org/10.1016/S0940-9602(98)80031-9
47. Stiles L, Shirihai OS. Mitochondrial dynamics and morphology in β-cells. Best Pract Res Clin Endocrinol Metab 2012; 26:725-38; PMID:23168275; http://dx.doi.org/10.1016/j.beem.2012.05.004
48. Lobanova ES, Herrmann R, Finkelstein S, Reidel B, Skiba NP, Deng WT, Jo R, Weiss ER, Hauswirth WW, Arshavsky VY. Mechanistic basis for the failure of cone transducin to translocate: why cones are never blinded by light. J Neurosci 2010; 30:6815-24; PMID:20484624; http://dx.doi.org/10.1523/JNEUROSCI.0613-10.2010
49. Holopigian K, Greenstein VC, Seiple W, Hood DC, Carr RE. Rod and Cone Photoreceptor Function in Patients with Cone Dystrophy. Invest Ophthal Vis Sci 2004; 45:275-81; PMID:14691184; http://dx.doi.org/10.1167/iovs.03-0627
50. Khan NW, Wissinger B, Kohl S, Sieving PA. CNGB3 achromatopsia with progressive loss of residual cone function and impaired rod-mediated function. Invest Ophthal Vis Sci 2007; 48:3864-71; PMID:17652762; http://dx.doi.org/10.1167/iovs.06-1521
51. Chang B, Dacey MS, Hawes NL, Hitchcock PF, Milam AH, Atmaca-Sonmez P, Nusinowitz S, Heckenlively JR. Cone photoreceptor function loss-3, a novel mouse model of achromatopsia due to a mutation in Gnat2. Invest Ophthal Vis Sci 2006; 47:5017-21; PMID:17065522; http://dx.doi.org/10.1167/iovs.05-1468
52. Xu J, Morris LM, Michalakis S, Biel M, Fliesler SJ, Sherry DM, Ding XQ. CNGA3 deficiency affects cone synaptic terminal structure and function and leads to secondary rod dysfunction and degeneration. Invest Ophthal Vis Sci 2012; 53:1117-29; PMID:22247469; http://dx.doi.org/10.1167/iovs.11-8168
53. Cho KI, Haque M, Wang J, Yu M, Hao Y, Qiu S, Pillai IC, Peachey NS, Ferreira PA. Distinct and atypical intrinsic and extrinsic cell death pathways between photoreceptor cell types upon specific ablation of Ranbp2 in cone photoreceptors. PLoS Genetics 2013; 9:e1003555; PMID:23818861; http://dx.doi.org/10.1371/journal.pgen.1003555
54. Rubinsztein DC, Codogno P, Levine B. Autophagy modulation as a potential therapeutic target for diverse diseases. Nat Rev Drug Discov 2012; 11:709-30; PMID:22935804; http://dx.doi.org/10.1038/nrd3802
55. Le YZ, Ash JD, Al-Ubaidi MR, Chen Y, Ma JX, Anderson RE. Targeted expression of Cre recombinase to cone photoreceptors in transgenic mice. Mol Vis 2004; 10:1011-8; PMID:15635292
56. Kuma A, Mizushima N. Chromosomal mapping of the GFP-LC3 transgene in GFP-LC3 mice. Autophagy 2008; 4:61-2; PMID:17786029; http://dx.doi.org/10.4161/auto.4846
57. Mattapallil MJ, Wawrousek EF, Chan CC, Zhao H, Roychoudhury J, Ferguson TA, Caspi RR. The Rd8 mutation of the Crb1 gene is present in vendor lines of C57BL/6N mice and embryonic stem cells, and confounds ocular induced mutant phenotypes. Invest Ophthal Vis Sci 2012; 53:2921-7; PMID:22447858; http://dx.doi.org/10.1167/iovs.12-9662
58. Heikkinen H, Nymark S, Koskelainen A. Mouse cone photoresponses obtained with electroretinogram from the isolated retina. Vision Res 2008; 48:264-72; PMID:18166210; http://dx.doi.org/10.1016/j.visres.2007.11.005
59. Nymark S, Heikkinen H, Haldin C, Donner K, Koskelainen A. Light responses and light adaptation in rat retinal rods at different temperatures. J Physiol 2005; 567:923-38; PMID:16037091; http://dx.doi.org/10.1113/jphysiol.2005.090662
60. Shi G, Yau KW, Chen J, Kefalov VJ. Signaling properties of a short-wave cone visual pigment and its role in phototransduction. J Neurosci 2007; 27:10084-93; PMID:17881515; http://dx.doi.org/10.1523/JNEUROSCI.2211-07.2007